Boundary Filter Optimization for Segmentation-Based Subband Coding

Alfred Mertins, *Member, IEEE*

Abstract—This paper presents boundary optimization techniques for the nonexpansive decomposition of arbitrary-length signals with multirate filterbanks. Both biorthogonal and paraunitary filterbanks are considered. The paper shows how matching moments and orthonormality can be imposed as additional conditions during the boundary filter optimization process. It provides direct solutions to the problem of finding good boundary filters for the following cases: a) biorthogonal boundary filters with exactly matching moments and b) orthonormal boundary filters with almost matching moments. With the proposed methods, numerical optimization is only needed if orthonormality and exactly matching moments are demanded. The proposed direct solutions are applicable to systems with a large number of subbands and/or very long filter impulse responses. Design examples show that the methods allow the design of boundary filters with good frequency selectivity.

Index Terms—Boundary filters, filterbanks, multirate signal processing, subband coding.

I. INTRODUCTION

MULTIRATE filterbanks are widely used in audio and image compression. On the encoder side, the signals are decomposed into subband signals that are then quantized, further compressed in a lossless manner, and stored or transmitted. The decoder reverses the lossless coding stage, feeds the quantized subband samples into a synthesis filterbank, and reconstructs an approximation of the original input signal. To keep the number of subband samples as low as possible critical subsampling is employed. Well-known applications are the MPEG audio standard [1] and wavelet-based image coding techniques such as JPEG-2000 [2].

While filterbanks are usually designed to process ongoing signals, it is also of significant interest to use them for the processing of finite-length signals, which occur for example in segmentation-based audio and in image coding. Segmentation-based audio coders divide an input signal into finite-length blocks and encode each block separately [3]–[5]. This strategy allows one to easily adapt the bit allocation to different signal segments and to directly access parts of the encoded bitstream. In addition, by segmenting audio signals directly in front of attacks, the problem of pre-echoes can be avoided [5]. Processing finite-length segments of a signal with multirate

filterbanks, however, requires some additional steps to ensure a nonexpansive decomposition where the total number of subband samples produced from a segment is equal to the number of input samples in that segment.

We assume a filterbank analysis with a uniform, critically sampled M-channel filterbank. The length of the input signal is denoted as N. The aim is to limit the total number of subband samples to N while being able to perfectly reconstruct the input signal from the subband samples. Several techniques to achieve this goal have been presented in the literature [5]–[17]. The oldest and simplest method to process finite-length signals is circular convolution [6], where finite-length signals are periodically extended prior filterbank analysis. If N is an integer multiple of M, the obtained subband signals are periodic with period N/M, and only M subband signals of length N/M need to be stored to enable exact reconstruction of the input signal. Because the left-hand side of a signal gets connected to the right-hand one, severe coding artifacts may occur when the signal properties are significantly different on both sides. A method with better properties is symmetric reflection, which has been studied by several authors [5], [7]–[10]. In this method, the finite-length signal is first symmetrically extended at its boundaries and then periodically extended, resulting in a signal with period $2N$ or $2N-2$, depending on the type of symmetry used for the extension. For certain constellations of N, M, extension symmetries, and in conjunction with linear-phase filters, symmetries in the subbands that allow us to achieve nonexpansive transforms can be obtained. An overview of permissible constellations is given in [10]. Finally, the use of boundary filters has been proposed in [11]–[18]. Using boundary filters means that the original filters of the filterbank are replaced by special filters at the boundaries of the signal that ensure that all of the information on a length-N input signal is contained in a total number of N subband samples. Interestingly, the above-mentioned methods of circular convolution and symmetric reflection can be interpreted as special forms of boundary filtering. However, boundary filters are not restricted to these cases. They can be applied to both nonlinear and linear-phase filterbanks with no restriction on the signal length.

In [11], [12], and [18] methods for the design of boundary filters are presented, but no direct solutions for their optimization are provided. In [14] and [17], numerical optimization has been employed. The work in [13] and [15] presents straightforward design methods for orthonormal boundary filters. However, desirable features such as matching moments are not included. The term "matching moments" means that the boundary filters match the moments of the stationary filters up to a certain degree. In [16], conditions for biorthogonal boundary filters with

$$\begin{bmatrix}
h_{\ell_0}(2)\,h_{\ell_0}(1)\,h_{\ell_0}(0) & & & & & & \\
h_{\ell_1}(2)\,h_{\ell_1}(1)\,h_{\ell_1}(0) & & & & & & \\
& h_0(3) & h_0(2) & h_0(1)\,h_0(0) & & & \\
& h_1(3) & h_1(2) & h_1(1)\,h_1(0) & & & \\
& & & h_0(3)\,h_0(2)\,h_0(1)\,h_0(0) & & \\
& & & h_1(3)\,h_1(2)\,h_1(1)\,h_1(0) & & \\
& & & & & h_{r_0}(3)\,h_{r_0}(2)\,h_{r_0}(1) \\
& & & & & h_{r_1}(3)\,h_{r_1}(2)\,h_{r_1}(1)
\end{bmatrix}$$

(a)

$$\begin{bmatrix}
h_{\ell_1}(1)\,h_{\ell_1}(0) & & & & & \\
h_0(3) & h_0(2) & h_0(1)\,h_0(0) & & & \\
h_1(3) & h_1(2) & h_1(1)\,h_1(0) & & & \\
& & h_0(3)\,h_0(2)\,h_0(1)\,h_0(0) & & \\
& & h_1(3)\,h_1(2)\,h_1(1)\,h_1(0) & & \\
& & & h_0(3)\,h_0(2)\,h_0(1)\,h_0(0) \\
& & & h_1(3)\,h_1(2)\,h_1(1)\,h_1(0) \\
& & & & h_{r_1}(3)\,h_{r_1}(2)
\end{bmatrix}$$

(b)

$$\begin{bmatrix}
g_{\ell_0}(1)\,g_{\ell_1}(1) & & & & \\
g_{\ell_0}(2)\,g_{\ell_1}(2)\,g_0(0)\,g_1(0) & & & \\
g_{\ell_0}(3)\,g_{\ell_1}(3)\,g_0(1)\,g_1(1) & & & \\
& g_0(2)\,g_1(2)\,g_0(0)\,g_1(0) & & \\
& g_0(3)\,g_1(3)\,g_0(1)\,g_1(1) & & \\
& & g_0(2)\,g_1(2)\,g_{r_0}(0)\,g_{r_1}(0) \\
& & g_0(3)\,g_1(3)\,g_{r_0}(1)\,g_{r_1}(1) \\
& & & g_{r_0}(2)\,g_{r_1}(2)
\end{bmatrix}$$

(c)

$$\begin{bmatrix}
g_{\ell_1}(2)\,g_0(0)\,g_1(0) & & & \\
g_{\ell_1}(3)\,g_0(1)\,g_1(1) & & & \\
& g_0(2)\,g_1(2)\,g_0(0)\,g_1(0) & & \\
& g_0(3)\,g_1(3)\,g_0(1)\,g_1(1) & & \\
& & g_0(2)\,g_1(2)\,g_0(0)\,g_1(0) \\
& & g_0(3)\,g_1(3)\,g_0(1)\,g_1(1) \\
& & & g_0(2)\,g_1(2)\,g_{r_0}(0) \\
& & & g_0(3)\,g_1(3)\,g_{r_0}(1)
\end{bmatrix}$$

(d)

Fig. 1. Example of size-limited analysis and synthesis matrices for two-band decompositions with $N = 8$ and length-4 filters: (a) and (b) Matrices $\boldsymbol{H}$ with different alignments relative to the input signal. (c) and (d) Synthesis matrices $\boldsymbol{G}$ corresponding to $\boldsymbol{H}$ as in (a) and (b), respectively.

vanishing moments were formulated for the two-channel case, but no direct solution was given. In [19], boundary filters for paraunitary filterbanks with ideal dc behavior and maximum coding gain were designed. However, no higher moments and no biorthogonal filterbanks were considered.

This paper presents novel solutions to the problem of optimizing the boundary filters for nonexpansive M-channel subband transforms. It shows how matching moments and orthonormality can be imposed as additional conditions during the boundary filter optimization process. Direct solutions are provided for the following cases: a) biorthogonal boundary filters with exactly matching moments and b) orthonormal boundary filters with almost matching moments. The solutions also include the simple cases where no moment conditions are imposed. The direct solutions are applicable to systems with a large number of subbands and/or very long filter impulse responses. The only case for which no straightforward solution is provided is the one where both orthonormality and exactly matching moments are demanded.

The paper is organized as follows. In Section II, the framework for the construction and manipulation of boundary filters is given. Section III shows how desired moment properties can be incorporated into the boundary filter construction. It also addresses the existence of solutions that yield both orthonormality and matching moments and states a test that allows us to check whether or not both properties can be simultaneously achieved. Methods for optimizing the boundary filters are presented in Section IV. Section V presents examples, and Section VI gives some conclusions.

II. FRAMEWORK FOR THE CONSTRUCTION OF BOUNDARY FILTERS

This section gives a matrix notation for the description of filterbank decompositions of finite-length signals and outlines the framework for the construction of boundary filters. We start by writing the subband decomposition of a signal $x(n)$ as

$$\boldsymbol{y} = \boldsymbol{H}\boldsymbol{x} \tag{1}$$

where the vector $\boldsymbol{x}$ contains the input sequence $x(n)$. $\boldsymbol{x}$ can be considered to be a length-N segment of an audio signal or a row or column of an image. $\boldsymbol{H}$ is an $N \times N$ matrix that describes the convolution of the input signal with the analysis filters and the downsampling operation. The vector $\boldsymbol{y}$ finally contains the subband samples.

There are many ways to define the structure of $\boldsymbol{y}$ and, thus, the structure of the transform matrix $\boldsymbol{H}$. Throughout this paper, we assume that the center part of $\boldsymbol{y}$, which is computed with the original filter impulse responses, has the form

$$[\ldots, y_0(n),\ldots, y_{M-1}(n), y_0(n+1),\ldots, y_{M-1}(n+1),\ldots]^T.$$

The definition of $\boldsymbol{y}$ at the boundaries depends on the signal length and the filter alignment used and will be specified as needed. Fig. 1(a) and (b) gives two examples of analysis matrices $\boldsymbol{H}$. As the examples show, the matrix rows in the center parts of $\boldsymbol{H}$ contain the time-shifted analysis impulse responses in reversed order. In the upper left and the lower right corners of the matrices, one finds the boundary filters whose impulse responses are different from the ones used in steady state. With respect to their position (left or right) these filters are denoted as $h_{l_0}(n)$, $h_{l_1}(n)$, $\ldots$, $h_{r_0}(n)$, $h_{r_1}(n)$. Note that the two examples consider the same signal length but use different filter alignments.

The synthesis operation can be written as

$$\hat{\boldsymbol{x}} = \boldsymbol{G}\boldsymbol{y} \tag{2}$$

with $\boldsymbol{G} = \boldsymbol{H}^{-1}$. The columns of $\boldsymbol{G}$ contain the synthesis filter impulse responses. Fig. 1(c) and (d) shows examples of the structure of $\boldsymbol{G}$.

The filter operations can be divided into three parts, namely, the processing of the left and right boundaries with boundary filters and the processing of the interior of the signal with the original filters. Correspondingly, the matrices can be partitioned as follows:

$$\boldsymbol{H} = \left[\boldsymbol{H}_1^T \,\middle|\, \boldsymbol{H}_2^T \,\middle|\, \boldsymbol{H}_3^T \right]^T$$
$$\boldsymbol{G} = [\boldsymbol{G}_1 | \boldsymbol{G}_2 | \boldsymbol{G}_3] \tag{3}$$

where $\boldsymbol{H}_1$ and $\boldsymbol{G}_1$ contain the boundary filters for the left-hand side, and $\boldsymbol{H}_3$ and $\boldsymbol{G}_3$ contain the ones for the right-hand side. The actual number of boundary filters and, thus, the number of rows of $\boldsymbol{H}_1$ and $\boldsymbol{H}_3$ depends on the number of subbands and the lengths of the filters.

For the analysis and synthesis operations, in partitioned form, we get

$$\boldsymbol{y}_k = \boldsymbol{H}_k \boldsymbol{x}, \quad \hat{\boldsymbol{x}} = \sum_{k=1}^{3} \boldsymbol{G}_k \boldsymbol{y}_k \tag{4}$$

where the vectors $\boldsymbol{y}_k$ are the corresponding partitions of $\boldsymbol{y}$.

If the perfect reconstruction (PR) condition $\boldsymbol{GH} = \boldsymbol{HG} = \boldsymbol{I}$ is satisfied, the submatrices satisfy $\boldsymbol{H}_k \boldsymbol{G}_j = \delta_{jk} \boldsymbol{I}_k$, where δ_{jk} denotes the Kronecker symbol, and matrices $\boldsymbol{I}_k$ are identity matrices of appropriate sizes. Terms of the form $\boldsymbol{G}_k \boldsymbol{H}_k$ describe projections (not necessarily orthogonal ones) onto the column space of $\boldsymbol{G}_k$. Clearly, if we want to replace one of the matrices $\boldsymbol{G}_k$ by a new (better) matrix $\tilde{\boldsymbol{G}}_k$, we also need to replace the corresponding analysis partition $\boldsymbol{H}_k$ by a new matrix $\tilde{\boldsymbol{H}}_k$, where both matrices have to satisfy $\tilde{\boldsymbol{H}}_k \tilde{\boldsymbol{G}}_k = \boldsymbol{I}_k$ and $\tilde{\boldsymbol{G}}_k \tilde{\boldsymbol{H}}_k = \boldsymbol{G}_k \boldsymbol{H}_k$. Hence, we see that both $\boldsymbol{G}_k$ and $\tilde{\boldsymbol{G}}_k$ must have the same column space, which has important consequences regarding the choice of $\tilde{\boldsymbol{G}}_k$. It means that the columns of $\tilde{\boldsymbol{G}}_k$ can be written as linear combinations of those of $\boldsymbol{G}_k$. With invertible, quadratic matrices $\boldsymbol{U}_k$, the linear combinations can be expressed as $\tilde{\boldsymbol{G}}_k = \boldsymbol{G}_k \boldsymbol{U}_k^{-1}$. For the analysis side, it means that $\tilde{\boldsymbol{H}}_k = \boldsymbol{U}_k \boldsymbol{H}_k$. Using the above-mentioned fact that $\boldsymbol{H}_k \boldsymbol{G}_j = \delta_{jk} \boldsymbol{I}_k$, it is easy to see that the modified matrices satisfy $\tilde{\boldsymbol{H}}_k \tilde{\boldsymbol{G}}_j = \boldsymbol{U}_k \boldsymbol{H}_k \boldsymbol{G}_j \boldsymbol{U}_j^{-1} = \delta_{jk} \boldsymbol{I}_k$.

The modified analysis and synthesis equations may be written as

$$\boldsymbol{v}_k = \tilde{\boldsymbol{H}}_k \boldsymbol{x}, \quad \hat{\boldsymbol{x}} = \sum_{k=1}^{3} \tilde{\boldsymbol{G}}_k \boldsymbol{v}_k \tag{5}$$

with

$$\tilde{\boldsymbol{H}}_k = \boldsymbol{U}_k \boldsymbol{H}_k, \quad \tilde{\boldsymbol{G}}_k = \boldsymbol{G}_k \boldsymbol{U}_k^{-1} \tag{6}$$

for $k = 1, 2, 3$. The matrix $\boldsymbol{U}_2$ is chosen as $\boldsymbol{U}_2 = \boldsymbol{I}_2$, which means that only the boundary filters are to be manipulated. The optimization of the boundary filters reduces to the optimization of $\boldsymbol{U}_1$ and $\boldsymbol{U}_3$, where all invertible matrices $\boldsymbol{U}_1$ and $\boldsymbol{U}_3$ satisfy the PR constraints. However, if we have a paraunitary filterbank and paraunitaryness is to be maintained, we have to restrict $\boldsymbol{U}_1$ and $\boldsymbol{U}_3$ to be orthogonal.

For extremely short segments, the boundary filters for the left and right boundaries merge, and $\boldsymbol{H}_2$ vanishes. In these cases,

we may replace $\boldsymbol{U}_1$ and $\boldsymbol{U}_3$ by a common matrix $\boldsymbol{U}$ such that $\boldsymbol{v} = \boldsymbol{UHx}$. Then, for each signal length N and required filter alignment, a dedicated matrix $\boldsymbol{UH}$ has to be implemented. The optimization of the matrices $\boldsymbol{U}$ can be carried out in the same way as the optimization of $\boldsymbol{U}_k$.

Initial solutions for the matrices $\boldsymbol{H}_1$, $\boldsymbol{H}_3$, $\boldsymbol{G}_1$, and $\boldsymbol{G}_3$ that guarantee PR can be found via the Gram–Schmidt procedure, as shown in [11]. To give a brief outline of this method, we consider a filterbank analysis described as $\boldsymbol{y} = \boldsymbol{Fx}_E$, where $\boldsymbol{y}$ contains the subband samples that are to be computed. The rows of $\boldsymbol{F}$ contain nontruncated, time-shifted, and flipped versions of the analysis filters' impulse responses. Note that $\boldsymbol{F}$ is rectangular in general and that the length of the input signal $\boldsymbol{x}_E$ is larger than the length of $\boldsymbol{y}$. The next step is to truncate $\boldsymbol{F}$ to an $N \times N$ matrix. Fig. 2 illustrates the truncation for a two-band decomposition and different cases of interest. The extension to the M-band case is straightforward. Given the truncated matrix, the method in [11] can be applied to design the required submatrices $\boldsymbol{H}_k$ and $\boldsymbol{G}_k$. The matrices $\boldsymbol{H}_2$ and $\boldsymbol{G}_2$ still contain the original impulse responses. The design method can be applied to both paraunitary and biorthogonal filterbanks. The result of the Gram–Schmidt procedure is somewhat arbitrary, and one cannot expect to design boundary filters with good properties this way; therefore, further optimization is needed. In the next two sections, methods for carrying out the optimization will be presented.

III. IMPOSING MOMENT CONDITIONS

One often aims at designing the analysis filters in a filterbank (or the wavelets used for a wavelet expansion) in such a way that they have a large number of vanishing moments because this ensures good energy compaction properties for low-order polynomial signals and other low-frequency signals. In the following, we assume that the analysis filters $h_k(n)$ in a given filterbank have a certain number of vanishing moments, and we look at the impact of boundary processing on the moment properties.

When applying a filterbank to a finite-length signal by using boundary filters, the problem that the boundary filters will usually not satisfy any moment conditions occurs, even if the original filters do. In the following, we will derive a method that enables us to partly match the moments of the boundary filters to the ones of the original filters in the filterbank. Our free design parameters are the elements of the matrices $\boldsymbol{U}_1$ and $\boldsymbol{U}_3$ so that we need to find restrictions on these matrices that guarantee the desired moment properties.

A. Matching Moments

We formulate the requirements of matching moments as

$$\boldsymbol{v}_k^{(i)} = \boldsymbol{U}_k \boldsymbol{y}_k^{(i)}, \quad i = 0, \ldots, \mu - 1, \qquad k = 1, 3 \tag{7}$$

with

$$\boldsymbol{y}_k^{(i)} = \boldsymbol{H}_k \boldsymbol{t}^{(i)}, \quad \boldsymbol{t}^{(i)} = \left[1^i, 2^i, \ldots, N^i \right]^T \tag{8}$$

$i = 0, \ldots, \mu - 1, k = 1, 3$, where μ denotes the number of conditions. The vectors $\boldsymbol{y}_k^{(i)}$ contain the actual filterbank responses

$$\begin{bmatrix} h_0(3) & \vdots & h_0(2) & h_0(1) & h_0(0) & & & & \\ h_1(3) & \vdots & h_1(2) & h_1(1) & h_1(0) & & & & \\ & & h_0(3) & h_0(2) & h_0(1) & h_0(0) & & & \\ & & h_1(3) & h_1(2) & h_1(1) & h_1(0) & & & \\ & & & & h_0(3) & h_0(2) & h_0(1) & \vdots & h_0(0) \\ & & & & h_1(3) & h_1(2) & h_1(1) & \vdots & h_1(0) \end{bmatrix}$$

(a)

$$\begin{bmatrix} h_1(3) & h_1(2) & \vdots & h_1(1) & h_1(0) & & & & \\ & & \vdots & h_0(3) & h_0(2) & h_0(1) & h_0(0) & & \\ & & \vdots & h_1(3) & h_1(2) & h_1(1) & h_1(0) & & \\ & & & & h_0(3) & h_0(2) & h_0(1) & h_0(0) & \\ & & & & h_1(3) & h_1(2) & h_1(1) & h_1(0) & \\ & & & & & h_0(3) & h_0(2) & h_0(1) & \vdots & h_0(0) \end{bmatrix}$$

(b)

$$\begin{bmatrix} h_0(3) & \vdots & h_0(2) & h_0(1) & h_0(0) & & & \\ h_1(3) & \vdots & h_1(2) & h_1(1) & h_1(0) & & & \\ & & h_0(3) & h_0(2) & h_0(1) & h_0(0) & & \\ & & h_1(3) & h_1(2) & h_1(1) & h_1(0) & & \\ & & & & h_0(3) & h_0(2) & \vdots & h_0(1) & h_0(0) \end{bmatrix}$$

(c)

$$\begin{bmatrix} h_1(3) & h_1(2) & \vdots & h_1(1) & h_1(0) & & & \\ & & \vdots & h_0(3) & h_0(2) & h_0(1) & h_0(0) & \\ & & \vdots & h_1(3) & h_1(2) & h_1(1) & h_1(0) & \\ & & & & h_0(3) & h_0(2) & h_0(1) & \vdots & h_0(0) \\ & & & & h_1(3) & h_1(2) & h_1(1) & \vdots & h_1(0) \end{bmatrix}$$

(d)

Fig. 2. Truncation of F for $M = 2$ bands. (a) and (b) Even-length signals of length six. (c) and (d) Odd-length signals of length five.

to polynomial input signals $t^{(i)}$, and the vectors $v_k^{(i)}$ contain the desired responses. Altogether, we may write

$$\underbrace{\left[v_k^{(0)}, v_k^{(1)}, \ldots, v_k^{(\mu-1)} \right]}_{V_k} = U_k \underbrace{\left[y_k^{(0)}, y_k^{(1)}, \ldots, y_k^{(\mu-1)} \right]}_{Y_k}$$
$$k = 1, 3. \qquad (9)$$

Example of the Choice of $v_k^{(i)}$: To give an example of the choice of $v_k^{(i)}$, we consider a two-channel filterbank, a dc signal $t^{(0)} = [1, \ldots, 1]^T$, and a vector y_1 defined as $y_1 = [y_0(0), y_1(0), y_0(1), y_1(1)]^T$. Assuming that $\sum_n h_0(n) = \sqrt{2}$ and $\sum_n h_1(n) = 0$, the desired response $v_1^{(0)}$ will typically be defined as $v_1^{(0)} = [\sqrt{2}, 0, \sqrt{2}, 0]^T$. This means that we aim at designing boundary lowpass and highpass filters with the same mean values as $h_0(n)$ and $h_1(n)$, respectively. In other words, the zero-order moments of the boundary filters are supposed to match the ones of the original filters. Following this idea, the desired responses $v_k^{(i)}$ for $i > 0$ can be defined according to the properties of $h_0(n)$ and $h_1(n)$ so that the boundary filters match the moment conditions of the original ones up to degree μ.

Given V_k and Y_k, the matrices U_k can be described (parameterized) as

$$U_k = U_k^o + P_k N_k^T \quad \text{with} \quad U_k^o = V_k Y_k^+, \qquad k = 1, 3 \tag{10}$$

where N_k contains a basis for the nullspace of Y_k such that $N_k^T Y_k = 0$. Matrix Y_k^+ is the pseudo inverse of Y_k, and P_k is an arbitrary matrix of appropriate size. If the number of conditions μ is small enough to ensure that $Y_k^+ Y_k = I_k$, the requirements (9) are fulfilled exactly. Provided that the nullspace contains more than just the null vector, the elements of P_k may be understood as free design parameters, which can be chosen to optimize U_k according to other criteria. If μ is so large that $Y_k^+ Y_k \neq I_k$, then (9) will be approximated in the least squares sense, and there will be no further free design parameters for optimization.

B. Increasing the Number of Free Design Parameters

Equation (9) is quite restrictive in the sense that the responses of all filters to the given input signals $t^{(i)}$ have to be specified. To have greater design freedom, we may want to specify only a few of these responses. For example, one might want the moments of some bandpass or highpass filters to vanish while imposing no restrictions on the moments of the lowpass filters. This can be achieved by deleting certain rows of (9). For the specified responses, this yields parameterizations of the form

$$U_k^{spec.} = U_k^{o, spec.} + P_k^{spec.} N_k^T, \qquad k = 1, 3 \tag{11}$$

where $U_k^{o, spec.}$ contains the corresponding rows of U_k^o defined in (10). For the nonspecified responses, we may freely choose the elements of matrices $U_k^{unspec.}$. Interleaving $U_k^{spec.}$ and $U_k^{unspec.}$ then yields U_k.

C. Orthonormality and Vanishing Moments

We now look at the problem of finding matrices U_k that satisfy both the moment conditions (9) and the orthonormality constraints

$$U_k^T U_k = I_k, \qquad k = 1, 3. \tag{12}$$

Such matrices are energy preserving so that (9) and (12) can only be satisfied simultaneously if the actual responses $y_k^{(i)}$, and the desired ones $v_k^{(i)}$ have equal energies: $\|v_k^{(i)}\|_2^2 = \|y_k^{(i)}\|_2^2$. If this condition is not satisfied *a priori* and orthonormality is desired, one must either change the requirements $v_k^{(i)}$ or prescale the boundary filters to meet the energy constraints.

If solutions to the problem (9) subject to (12) exist, then one of them is given by $U_k = A_k B_k^T$, where $A_k^T [V_k Y_k^T] B_k = \Sigma_k$ is the singular value decomposition (SVD) of $V_k Y_k^T$. The matrices $U_k, k = 1, 3$ computed this way are the solutions to the subspace rotation (Procrustes) problems

$$\text{minimize} \ \|V_k - U_k Y_k\|_F \quad \text{s.t.} \quad U_k^T U_k = I_k$$

where $\| \cdot \|_F$ denotes the Frobenius norm [20]. If $\|V_k - U_k Y_k\|_F = 0$, then the conditions are satisfied exactly. The measure $\|V_k - U_k Y_k\|_F$ with $U_k = A_k B_k^T$ from above can

be used as a test to find out whether or not both (9) and (12) can be satisfied simultaneously.

Clearly, with an increasing number of conditions on U_k, the solution space decreases, and it might be impossible to satisfy both (9) and (12). For the simple case $V_k = v_k^{(0)}$ and $Y_k = y_k^{(0)}$, however, orthogonal matrices U_k generally exist as long as $\|v_k^{(0)}\|_2^2 = \|y_k^{(0)}\|_2^2$. Finding the optimal matrices U_k with respect to a given criterion and subject to (9) and (12) is yet another problem that generally requires numerical optimization. However, a method that allows the moment conditions to be satisfied approximately (with sufficiently high precision for practical purposes) while yielding a direct solution to the optimization problem will be presented in Section IV-E.

IV. OBJECTIVE FUNCTION AND BOUNDARY FILTER OPTIMIZATION

We assume that a filterbank has been chosen for a given application (e.g., audio or image coding) because of its good properties. When applying the filterbank to a finite-length input signal, the boundary filters should have similar properties as the filters used in steady state. If this is the case, the same bit allocation can be used at the boundaries and in the interior of the signal, which is quite desirable from a practical point of view. If the filter energies vary significantly in the boundary regions, a temporal adjustment of the bit allocation (or spatial adjustment in the 2-D case) is needed to avoid effects like spatially varying noise when reconstructing the signal from its quantized subband coefficients. Adjusting the bit allocation to avoid such effects has been proposed in [21]. In this paper, we design boundary filters in such a way that their properties become most similar to those of the original filters so that an adjustment of the bit allocation can be avoided.

A. Objective Function

To explain the motivation behind the proposed method, we consider a length-N vector of subband samples computed as

$$w = Fx_E$$

where F is as in Section II and x_E is a stationary input process. The matrix F, whose rows contain time-shifted, nontruncated versions of the analysis filter impulse responses, describes the filterbank analysis in steady state. Consequently, the input vector x_E must be longer than w whenever the filter length is larger than M. We now look at a length-N part in the center of x_E, denote it as x, and describe its analysis as

$$v = UHx$$

where v has length N. The vector x can be written as $x = Cx_E$, where C describes the truncation so that v can alternatively be written as

$$v = UHCx_E.$$

The aim is to minimize the error measure $E\{\|v-w\|^2\}$ for given input statistics through the choice of U. This means that we want to make the subband samples computed from the truncated
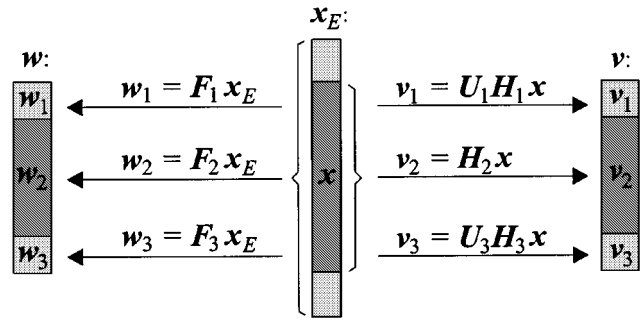

Fig. 3. Computation of w_k and v_k from x_E.

signal x as close as possible to the ones computed from the longer signal x_E.

By partitioning the vectors into three parts, according to the description in Section II, we can formulate objective functions

$$\phi(U_k) = E\left\{\|v_k - w_k\|^2\right\}, \qquad k = 1, 3 \qquad (13)$$

where $v_k = U_k H_k C x_E$ and $w_k = F_k x_E$ with $F = [F_1^T | F_2^T | F_3^T]^T$. Fig. 3 gives an illustration of the concept. The objective functions finally become

$$
\begin{aligned}
\phi(U_k) &= E\left\{\|[U_k H_k C - F_k] x_E\|^2\right\} \\
&= \mathrm{tr}\left\{[U_k H_k C - F_k] R_{xx} [U_k H_k C - F_k]^T\right\} \\
&\qquad k = 1, 3 \qquad\qquad\qquad\qquad\qquad (14)
\end{aligned}
$$

where R_{xx} is the autocorrelation matrix of the process x_E, and $\mathrm{tr}\{\}$ denotes the trace of a matrix. Given R_{xx}, H_k, and C, the aim is to minimize $\phi(U_k)$ through the choice of U_k, $k = 1, 3$.

B. Unrestricted Optimization

If no restrictions on U_k are imposed, minimizing $\phi(U_k)$ is straightforward. The optimal matrix U_k is found to be

$$U_k = F_k R_{xx} C^T H_k^T \left[H_k C R_{xx} C^T H_k^T\right]^{-1}. \qquad (15)$$

To see this, we replace U_k in (14) with $U_k + \Delta$, where Δ is an arbitrary matrix, and insert U_k according to (15) into the expression obtained. We get

$$
\begin{aligned}
\phi(U_k) = \mathrm{tr}\Big\{&F_k R_{xx} F_k^T - F_k R_{xx} C_k^T H_k^T \\
&\cdot \left[H_k C_k R_{xx} C_k^T H_k^T\right]^{-1} H_k C_k R_{xx} F_k^T \\
&+ \Delta H_k C_k R_{xx} C_k^T H_k^T \Delta^T\Big\}. \qquad (16)
\end{aligned}
$$

Clearly, the minimum of (16) occurs for $\Delta = 0$, which shows that (15) is the optimum solution to the given problem.

C. Including Moment Conditions

To include moment conditions during the boundary filter optimization, we parameterize U_k in the form $U_k = V_k Y_k^+ + P_k N_k^T$, as described in Section III-A. The objective function (14) then becomes

$$
\begin{aligned}
\phi(U_k) = \Big\{&\left[P_k N_k^T H_k C_k + V_k Y_k^+ H_k C_k - F_k\right] R_{xx} \\
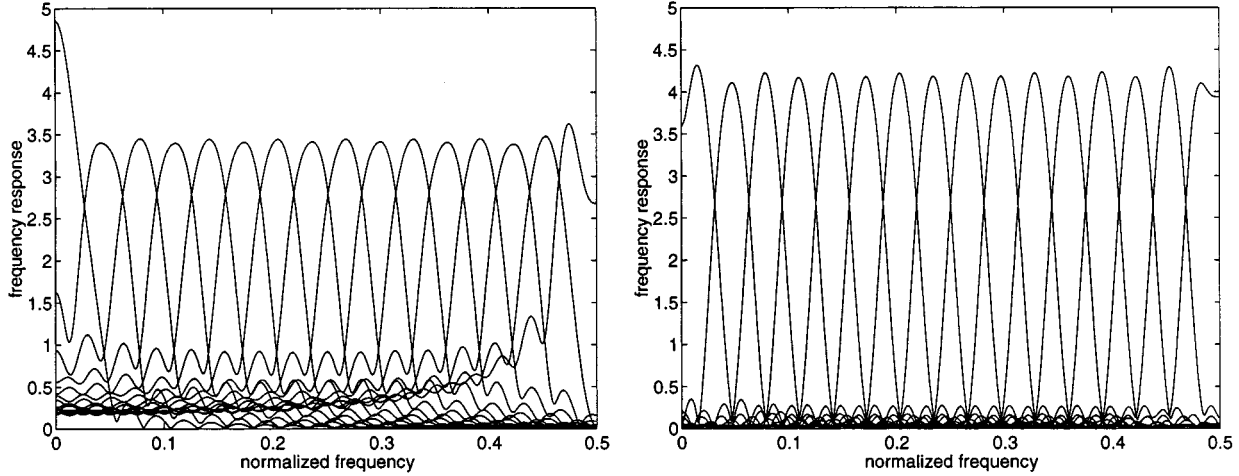&\cdot \left[P_k N_k^T H_k C_k + V_k Y_k^+ H_k C_k - F_k\right]^T\Big\}. \qquad (17)
\end{aligned}
$$

Fig. 4. Frequency responses of boundary analysis filters designed via Gram–Schmidt method. Parameters: $M = 16$, ELT prototype, 32 boundary filters. Left: $h_{\ell,0}(n), \ldots, h_{\ell,15}(n)$. Right: $h_{\ell,16}(n), \ldots, h_{\ell,31}(n)$.

Using the same arguments as above, one can show that the optimal parameter matrix P_k is given by

$$P_k = \left[F_k - V_k Y_k^+ H_k C \right] R_{xx} C^T H_k^T N_k$$
$$\cdot \left[N_k^T H_k C R_{xx} C^T H_k^T N_k \right]^{-1}. \qquad (18)$$

D. Imposing Orthonormality

For paraunitary filterbanks where we demand that matrices U_k are orthogonal, the optimal matrices according to (14) can be found via SVDs [13]. To derive the solution, we consider R_{xx} to be decomposed into $R_{xx} = LL^T$ (for example, a Cholesky decomposition). The optimization problem may then be written as a set of subspace rotation problems [20]:

$$\text{minimize } \|[U_k H_k C - F_k]L\|_F^2 \quad \text{s.t.} \quad U_k^T U_k = I_k$$
$$k = 1, 3. \qquad (19)$$

To solve (19), we compute the SVDs

$$A_k \Sigma_k B_k^T = \left[H_k C L L^T F_k^T \right]^T = \left[H_k C R_{xx} F_k^T \right]^T \qquad (20)$$

and find the final solutions as

$$U_k = A_k B_k^T, \qquad k = 1, 3. \qquad (21)$$

E. Orthonormality and Almost Vanishing Moments

If both orthonormality and matching moments are to be achieved exactly, numerical optimization may be used. In this section, we slightly relax the conditions and look for solutions that maintain orthonormality but satisfy the moment conditions only approximately.

We assume that the moment conditions are stated in such a way that an orthonormal solution exists. That is, the problem $U_k Y_k = V_k$ is supposed to have a solution with an orthogonal matrix U_k. We use the objective function (19) and amend it with the additional moment conditions as follows:

$$\text{minimize } \|[U_k \mathcal{H}_k - \mathcal{F}_k]\mathcal{L}\|_F^2 \quad \text{s.t.} \quad U_k^T U_k = I_k, \quad k = 1, 3 \qquad (22)$$

with

$$\mathcal{H}_k = [H_k C, Y_k],; \; \mathcal{F}_k = [F_k, V_k], \; \mathcal{L} = \begin{bmatrix} L & 0 \\ 0 & \lambda I \end{bmatrix}. \qquad (23)$$

The solutions then becomes

$$U_k = A_k B_k^T, \qquad k = 1, 3 \qquad (24)$$

where A_k and B_k are taken from the SVDs

$$A_k \Sigma_k B_k^T = \left[\mathcal{H}_k \mathcal{L} \mathcal{L}^T \mathcal{F}_k^T \right]^T. \qquad (25)$$

V. EXAMPLES

In the first example, we consider a paraunitary, cosine-modulated 16-band filterbank with extended lapped transform (ELT) prototype according to [22]. In this filterbank, the subband filters have nonlinear phase so that symmetric reflection techniques cannot be applied, and boundary filters must be used. The filter length of an ELT is $4M$. The filter alignment for processing finite-length signals is chosen such that there are $2M$ boundary filters on each side of a signal of length KM, where K is an integer. The vector of subband samples is defined as

$$\boldsymbol{y} = [y_0(0), \ldots, y_{M-1}(0), \ldots \ldots, y_0(K-1), \ldots$$
$$y_{M-1}(K-1)]^T.$$

The initial boundary filters were designed via the Gram–Schmidt procedure. The frequency responses of the boundary filters (left boundary) are depicted in Fig. 4. In this example, the Gram–Schmidt procedure directly yields boundary filters with relatively good frequency selectivity. However, a weakness of the method is that several boundary filters, in addition to the lowpass ones, have large nonzero mean. Thus, when processing signals with a large dc component (for example, in image compression), a significant amount of the dc component will leak into several bands and may cause problems with the bit allocation in these bands.

Fig. 5 shows the frequency responses of the boundary filters designed with the biorthogonal method proposed in Section IV-C. The filters were parameterized according to (9) to
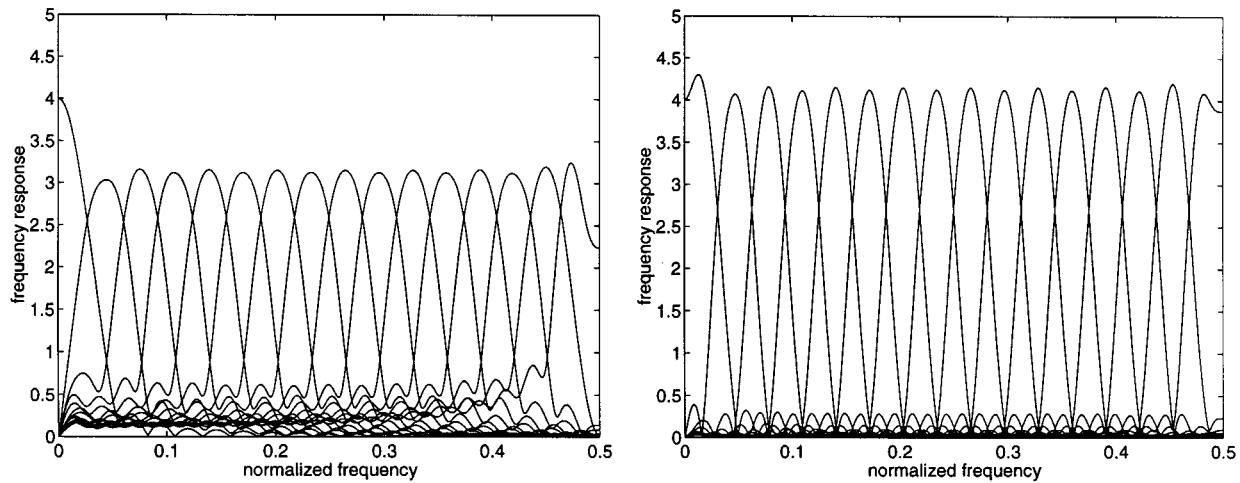
Fig. 5. Frequency responses of biorthogonal boundary analysis filters designed with the algorithm in Section IV-C. Parameters as in Fig. 4; one vanishing moment. Left: $h_{\ell,0}(n), \ldots, h_{\ell,15}(n)$. Right: $h_{\ell,16}(n), \ldots, h_{\ell,31}(n)$.
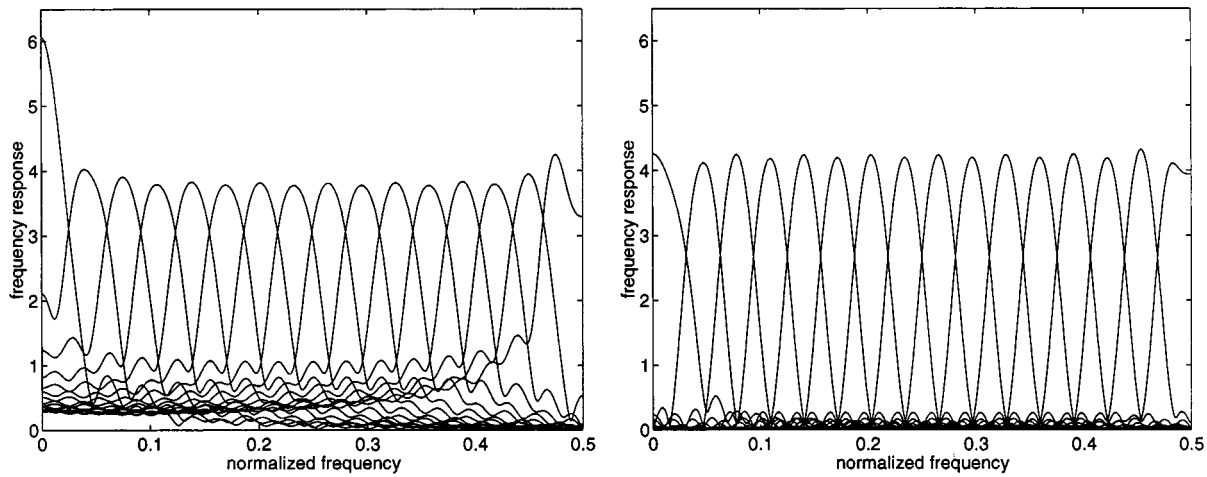

Fig. 6. Frequency responses of boundary synthesis filters, corresponding to the analysis in Fig. 5. Left: $g_{\ell,0}(n), \ldots, g_{\ell,15}(n)$. Right: $g_{\ell,16}(n), \ldots, g_{\ell,31}(n)$.
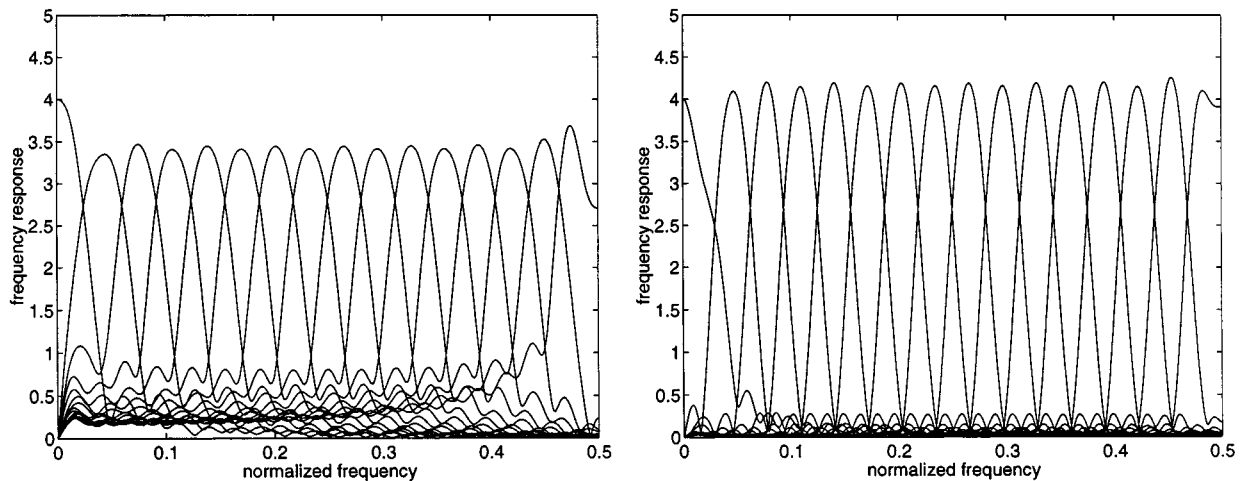

Fig. 7. Frequency responses of orthogonal boundary analysis filters designed with the algorithm in Section IV-E. Parameters as in Fig. 4; near-ideal dc behavior. Left: $h_{\ell,0}(n), \ldots, h_{\ell,15}(n)$. Right: $h_{\ell,16}(n), \ldots, h_{\ell,31}(n)$.

have one matching moment. During optimization, a white noise input process was considered. The plots in Fig. 5 show that the resulting filters have ideal behavior for dc signals and good frequency selectivity.
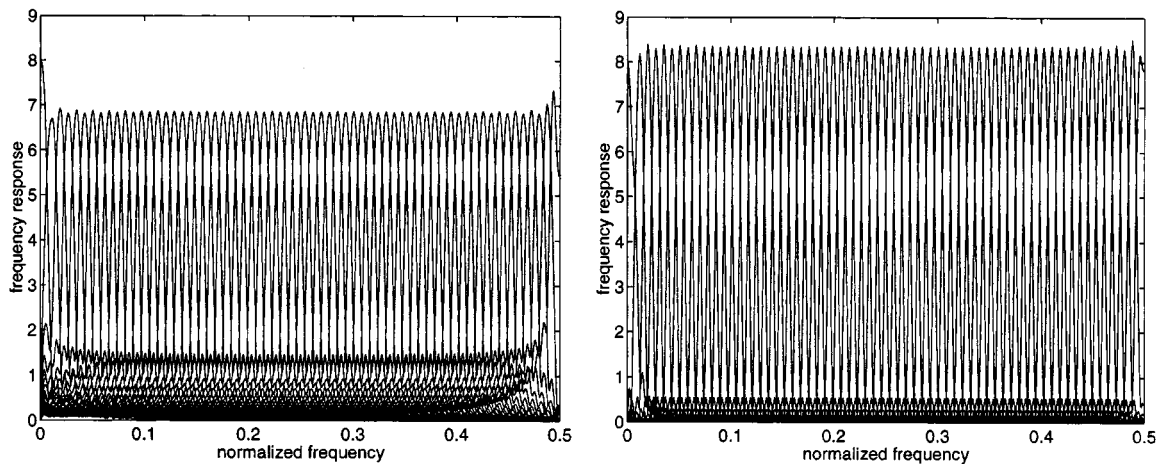
Fig. 8. Frequency responses of orthogonal boundary analysis filters with near-perfect dc behavior. Parameters: $M = 64$, ELT prototype, 128 boundary filters. Left: $h_{\ell,0}(n), \ldots, h_{\ell,63}(n)$. Right: $h_{\ell,64}(n), \ldots, h_{\ell,127}(n)$.
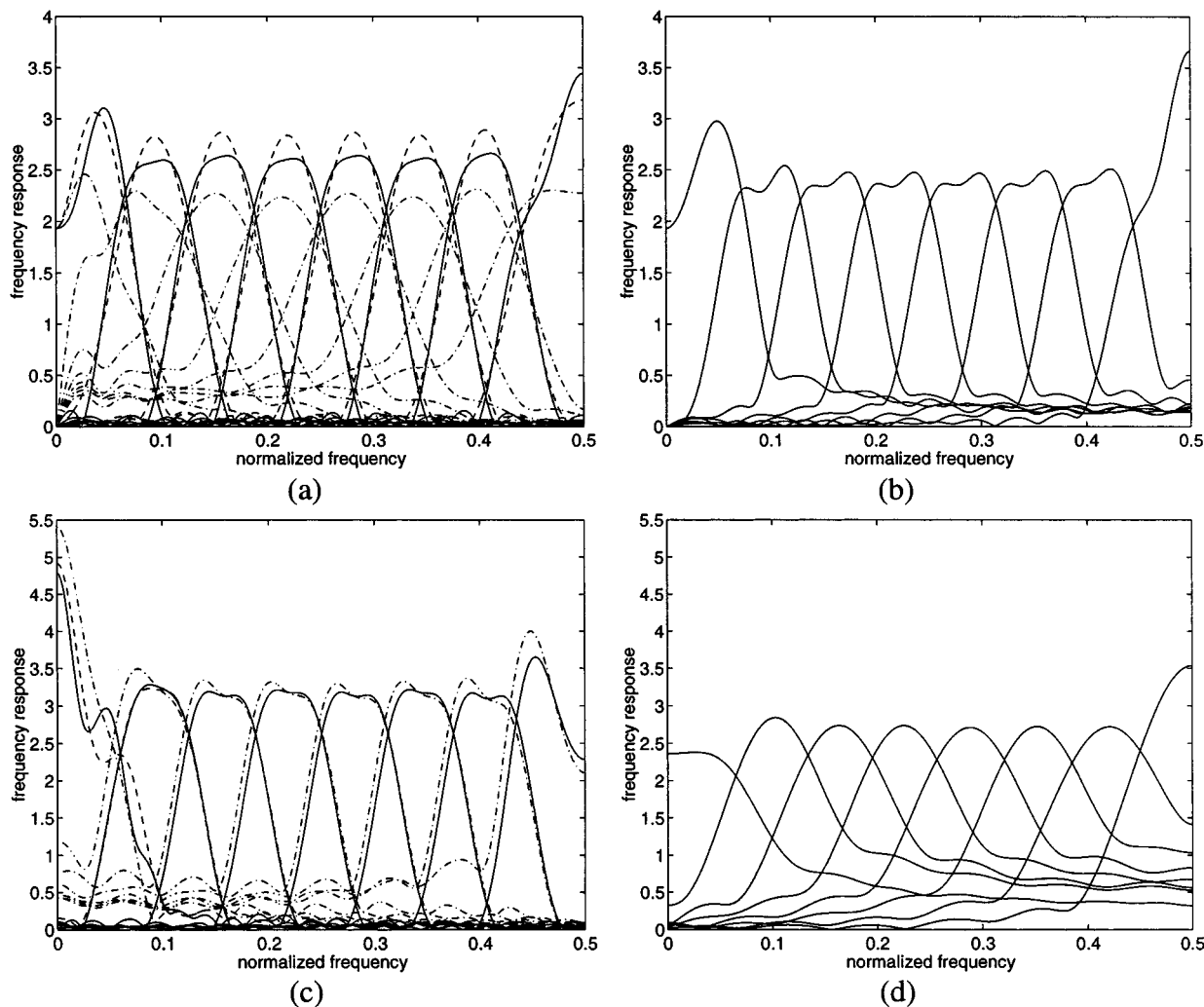

Fig. 9. Frequency responses of biorthogonal boundary filters with one matching moment, designed with the algorithm in Section IV-C. (a) Analysis filters for left-hand side. (b) Analysis filters for right-hand side. (c) Synthesis filters for left-hand side. (d) Synthesis filters for right-hand side.

Since the filter optimization considers only the analysis side, it is not guaranteed that the synthesis boundary filters, although providing perfect reconstruction, are frequency selective and behave as desired. To demonstrate that the synthesis boundary filters have good properties, their frequency responses are de-

picted in Fig. 6. These filters, however, do not have vanishing moments.

Boundary filters for the given filterbank example were also designed with the unrestricted and the orthonormal methods outlined in Sections IV-B and D. The results, however, do not

differ much from the ones obtained with the Gram–Schmidt method and are not plotted explicitly. Essentially, both of these methods result in dc leakage into several bands.

Finally, orthogonal boundary filters with almost perfect dc behavior were designed. For this, the required dc responses $\boldsymbol{v}_k^{(0)}$ had to be prescaled to meet the energy of the given dc responses $\boldsymbol{y}_k^{(0)}$. The optimization was then carried out as described in Section IV-E. The obtained lowpass boundary filters were finally scaled to meet the desired dc responses exactly. Therefore, the lowpass boundary filters' energies are not equal to one. They are 0.7746 for the analysis and 1/0.7746 for the corresponding synthesis filters. All other filters have unit energy. The frequency responses of the optimized analysis filters are depicted in Fig. 7. The maximum dc amplification of the nonlowpass bands is on the order of 10^{-10} and can be regarded as practically ideal. Since the solution is orthogonal, the frequency responses of the synthesis filters are the same as for the analysis ones, apart from scaling of the lowpass filters.

To show that larger problems can be tackled with the proposed methods, boundary filters for a 64-channel filterbank were designed. Again, an ELT was used. The frequency responses of orthogonal boundary filters with near perfect dc behavior are depicted in Fig. 8. The maximum dc amplification of nonlowpass bands is in the order of 10^{-10} and, thus, practically ideal. As before, the energies of the analysis lowpass filters are 0.7746 due to scaling. Boundary filters with comparable frequency responses were obtained with the biorthogonal method from Section IV-C under the constraint of an ideal dc behavior.

In a final example, we consider an eight-channel, biorthogonal, low-delay, cosine-modulated filterbank with a filter length of $L = 32$ and a system delay of 15 taps. The prototype is designed to have no dc leakage [23]. The signal length N is chosen to be an integer multiple of the number of channels. Because low-delay filters have most of their energy concentrated at the beginning of their impulse responses, it turned out to be advantageous to set up $\boldsymbol{H}$ in such a way that different numbers of boundary filters are used on both sides. Therefore, $3M$ boundary filters were designed for the left-hand side, whereas only M were used on the right-hand side. The boundary filters for the PR analysis/synthesis system were designed with the algorithm in Section IV-C under the constraint of an ideal dc behavior. The frequency responses of the boundary analysis filters are depicted in Fig. 9(a) and (b). Note that Fig. 9(a) shows the frequency responses of all $3M$ boundary filters for the left-hand side, where three filters always have the same passband. All analysis filters have good frequency selectivity, and as required, they have an ideal dc behavior. Fig. 9(c) and (d) depict the frequency responses of the boundary synthesis filters. In addition, these filters are sufficiently frequency selective.

VI. CONCLUSIONS

In this paper, closed-form solutions for the design of optimal boundary filters for processing finite-length signals with filterbanks have been presented. The boundary filters are designed in such a way that they have the same moments (up to a certain degree) as the original filters in the filterbank. The proposed methods ensure a minimum number of subband samples and are applicable to both paraunitary and biorthogonal filterbanks. Design examples have been presented for cosine-modulated filterbanks, as often used in audio compression. It turned out that the designed boundary filters have a good frequency selectivity so that good coding properties can be expected.

REFERENCES

[1] Int. Org. Standardiz., "Coding of Moving Pictures and Associated Audio for Digital Storage Media at up to about 1.5 MBit/s, Audio Part (11172-3),", Nov. 1992.

[2] Joint photographic experts group. (2000) JPEG2000 Final Committee Draft. [Online]. Available: http://www.jpeg.org

[3] J. Princen and J. D. Johnston, "Audio coding with signal adaptive filterbanks," in *Proc. IEEE Int. Conf. Acoust., Speech, Signal Process.*, Detroit, MI, 1995, pp. 3071–3074.

[4] D. Sinha and J. D. Johnston, "Audio compression at low bit rates using a signal adaptive switched filterbank," in *Proc. IEEE Int. Conf. Acoust., Speech, Signal Process.*, vol. 2, Atlanta, GA, 1996, pp. 1053–1056.

[5] J. Kliewer and A. Mertins, "Audio subband coding with improved representation of transient signal segments," in *Proc. Euro. Signal Process. Conf.*, Rhodos, Greece, Sept. 1998, pp. 2345–2348.

[6] J. Woods and S. O'Neil, "Subband coding of images," *IEEE Trans. Acoust., Speech, Signal Processing*, vol. ASSP-34, pp. 1278–1288, May 1986.

[7] M. J. T. Smith and S. L. Eddins, "Analysis/synthesis techniques for subband coding," *IEEE Trans. Acoust., Speech, Signal Processing*, vol. 38, pp. 1446–1456, Aug. 1990.

[8] J. N. Bradley, C. M. Brislawn, and V. Faber, "Reflected boundary conditions for multirate filterbanks," in *Proc. Int. Symp. Time-Freq. Time-Scale Anal.*, Banff, AB, Canada, 1992, pp. 307–310.

[9] H. J. Barnard, J. H. Weber, and J. Biemond, "Efficient signal extension for subband/wavelet decomposition of arbitrary length signals," *Proc. SPIE, VCIP*, vol. 2094, pp. 966–975, Nov. 1993.

[10] L. Chen, T. Q. Nguyen, and K. P. Chan, "Symmetric extension methods for M-channel linear-phase perfect reconstruction filterbanks," *IEEE Trans. Signal Processing*, vol. 43, pp. 2505–2511, Nov. 1995.

[11] C. Herley, "Boundary filters for finite-length signals and time-varying filterbanks," *IEEE Trans. Circuits Syst. II*, vol. 42, pp. 102–114, Feb. 1995.

[12] R. L. de Queiroz, "Subband processing of finite length signals without border distortions," in *Proc. IEEE Int. Conf. Acoust., Speech, Signal Process.*, vol. IV, San Francisco, CA, Mar. 1992, pp. 613–616.

[13] A. Mertins, "Time-varying and support preservative filterbanks: Design of optimal transition and boundary filters via SVD," in *Proc. IEEE Int. Conf. Acoust., Speech, Signal Process.*, Detroit, MI, May 1995, pp. 1316–1319.

[14] R. L. de Queiroz and K. R. Rao, "Optimal orthogonal boundary filterbanks," in *Proc. IEEE Int. Conf. Acoust., Speech, Signal Process.*, vol. II, Detroit, MI, May 1995, pp. 1296–1299.

[15] T. Kalker, "On optimal boundary and transition filters in time-varying filterbanks," in *Proc. IEEE Int. Conf. Image Process.*, vol. 1, 1996, pp. 625–628.

[16] M. Coffey, "Boundary compensated wavelet bases," in *Proc. IEEE Int. Conf. Acoust., Speech, Signal Process.*, München, Germany, May 1997, pp. 2129–2132.

[17] A. Mertins, "Optimized biorthogonal shape adaptive wavelets," in *Proc. IEEE Int. Conf. Image Process.*, vol. 3, Chicago, IL, Oct. 1998, pp. 673–677.

[18] C. Herley, J. Kovačević, K. Ramchandran, and M. Vetterli, "Tilings of the time-frequency plane: construction of arbitrary orthogonal bases and fast tiling algorithms," *IEEE Trans. Signal Processing*, vol. 41, pp. 3341–3359, Dec. 1993.

[19] A. Mertins, "Boundary filters for size-limited paraunitary filterbanks with maximum coding gain and ideal DC behavior," *IEEE Trans. Circuits Syst. II*, vol. 48, pp. 183–188, Feb. 2001.

[20] G. H. Golub and C. F. Van Loan, *Matrix Computations*, 3rd ed. Baltimore, MD: John Hopkins Univ. Press, 1996.

[21] V. Nuri and R. H. Bamberger, "Size limited filterbanks for subband image compression," *IEEE Trans. Image Processing*, vol. 4, pp. 1317–1323, Sept. 1995.

[22] H. S. Malvar, "Extended lapped transforms: Fast algorithms and applications," *IEEE Trans. Signal Processing*, vol. 40, pp. 2703–2714, Nov. 1992.

[23] T. Karp and A. Mertins, "Biorthogonal cosine-modulated filterbanks without DC leakage," in *Proc. IEEE Int. Conf. Acoust., Speech, Signal Process.*, vol. 3, Seattle, WA, May 1998, pp. 1457–1460.

Alfred Mertins (M'95) received the Dipl.-Ing. degree from the University of Paderborn, Paderborn, Germany, in 1984 and the Dr.-Ing. degree in electrical engineering and the Dr.-Ing. habil. degree in telecommunications from the Hamburg University of Technology, Hamburg, Germany, in 1991 and 1994, respectively.

From 1986 to 1991, he was with the Hamburg University of Technology, from 1991 to 1995, with the Microelectronics Applications Center, Hamburg, from 1996 to 1997, with the University of Kiel, Kiel, Germany, and from 1997 to 1998, with the University of Western Australia, Nedlands, Australia. Since 1998, he has been with the School of Electrical, Computer and Telecommunications Engineering, University of Wollongong, Wollongong, Australia. His research interests include digital signal processing, wavelets and filterbanks, image and video processing, and digital communications.